

Enhanced optical transmission through a nanoslit by coupling light between periodic strips and metal film

Huajun Zhao (赵华君)* and Dairong Yuan (袁代蓉)

Department of Electronic and Electrical Engineering, Chongqing University of Arts and Sciences, Chongqing 402160, China

*E-mail: zhaohjcu@163.com

Received May 20, 2010

Surface plasmon resonance (SPR) is obtained by exciting the surface plasmon (SP) at the metal and dielectric interface, which can greatly enhance the extraordinary optical transmission (EOT) through a nanoslit milled in the metal film. We present a structure with a 50-nm-wide silver nanoslit for EOT by coupling light into the dielectric interlayer between periodic strips and a metal film. When the period of the metallic strips is equal to the wavelength of the SPR, the transmission efficiency of 187.6 through the nanoslit is enhanced. The metallic strip width over the nanoslit is optimized to improve transmission efficiency, and the maximal efficiency of 204.3 is achieved.

OCIS codes: 240.6680, 310.6628, 050.1220.

doi: 10.3788/COL20100812.1117.

Since Ebbesen *et al.* experimentally demonstrated that arrays of nanoholes^[1] and nanoslits^[2] in metal films have extraordinary optical transmission (EOT), the physical mechanisms and applications of enhanced transmissions were intensively investigated^[3,4]. Transmission efficiency can significantly increase due to the role of the surface plasmon (SP) excited at the interface between metals and dielectric materials^[5,6]. The excitation of SP by light is denoted as a surface plasmon resonance (SPR) that propagates along the metal and dielectric interface^[7,8]. The corrugations can increase the light-plasmon coupling^[9,10] when the metal surface surrounding the aperture has periodic corrugations^[2,11]. Furthermore, if the Fabry-Perot cavity resonance is formed in a nanohole or nanoslit (i.e., waveguide cavity) for interference^[12], the EOT can be enhanced.

In this letter, the structure of enhanced EOT in a metal nanoslit by coupling light between periodic strips and a metal film is presented, as shown in Fig. 1. The structure features a metal film with thickness t , a nanoslit with width w_p , a dielectric film with thickness d , a metal strip above the slit with width L , and n periods on each side with period width A , ridge width w_s , and depth h . Both the metal film and the strips are made of silver with permittivity $\epsilon_{Ag} = -48.8 + 3.16i$ ^[13]. The dielectric interlayer between the periodic strips and the metal film is fused silica, whose permittivity is $\epsilon_d = 2.1$. For a normal incident transverse magnetic (TM) polarized plane wave with wavelength of $1.0 \mu\text{m}$, the transmission efficiency η of the slit is defined as the ratio of the total energy transmitted to the far field to the energy incident on the slit without the strips and the dielectric spacer layer. The total energy transmitted to the far field is the z -component \mathbf{S}_z of the time-averaged Poynting vector $\mathbf{S} = 1/2 \text{Real}(\mathbf{E} \times \mathbf{H}^*)$ multiplied by the slit-width w_s . To address the optimal corrugation geometry of the structure, the influence of the geometry parameters on transmission efficiency was discussed. All the results were calculated by rigorous coupled wave analysis (RCWA) method^[14,15]. A perfect matched layer (PML) was applied to avoid artificial reflections from the

boundaries of the studied domain, and the validity was confirmed by comparing the results of the structures in Refs. [16] and [17].

The wavelength of the SPR at an interface between a semi-infinite metal and dielectric materials is $\lambda_{sp} = \text{Re}[(\lambda_0 / \sqrt{\epsilon_{Ag}\epsilon_d / (\epsilon_{Ag} + \epsilon_d)})] \approx 675 \text{ nm}$. Here, $\lambda_0 = 1.0 \mu\text{m}$ is the incident light wavelength, and ϵ_{Ag} and ϵ_d are the permittivities of silver and fused silica, respectively. To obtain the normal incident TM polarized light coupling with SP, the pitch or periodicity should be matched with the SP wavelength for periodic corrugation^[5,18]. The transmission efficiency η through a nanoslit as a function

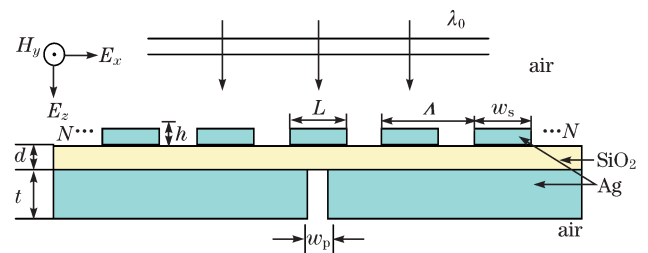


Fig. 1. Schematic structure of EOT through a nanoslit by coupling light between the periodic strips and a metal film.

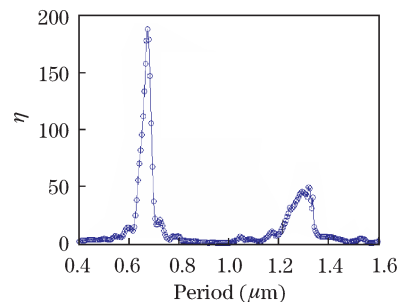


Fig. 2. Transmission efficiency η through a 50-nm-wide nanoslit as a function of the periods of metallic strips for a normal incident TM polarized plane wave with wavelength of $1.0 \mu\text{m}$. $t = 250 \text{ nm}$, $h = 90 \text{ nm}$, $d = 180 \text{ nm}$, $L = 475 \text{ nm}$, $w_s = 475 \text{ nm}$, $w_p = 50 \text{ nm}$, $\lambda_0 = 1.0 \mu\text{m}$, and $N = 12$.

of the period is shown in Fig. 2. When the period of the metal strips is about 675 nm, which is equal to the SP wavelength λ_{sp} , the maximum transmission efficiency of 187.6 through the nanoslit is obtained, which is about 24 times than that of the bare resonant nanoslit ($\eta=7.8$)^[4]; efficiency is also larger than the nano-cavity antenna array for EOT ($\eta=128.3$)^[19]. When the period of the metal strips is close to twice the SP wavelength (i.e., $\Lambda \approx 1350$ nm), there is a larger transmission efficiency, as shown in Fig. 2. The physical mechanism of EOT can be interpreted as a result of charge displacement in the metal film near the metal and dielectric interface. Figure 3 shows the surface charge distribution and the electric fields associated with the EOT structure. The array of metal strips provided a phase-matching condition for exciting SP at the silver/silica interface in the metal film, transforming the incident light into the dielectric interlayer. When the SP is excited, alternating positive/negative charges near the top surface of the metallic film are produced, as shown in Fig. 3. Furthermore, the incident plane wave transformed into a strong localized surface plasmon wave (SPW) in the dielectric interlayer. The exciting of SPW at the silver/silica interface constructively interfered within the dielectric interlayer waveguide and provided the enhanced EOT in the nanoslit. Indeed, when $\Lambda = n \times \lambda_{sp}$ (where n is an integer, and λ_{sp} is the SP wavelength transmitted along the dielectric interlayer between the periodic strips and the metal film), the transmission of light through the nanoslit is maximal for $\Lambda \approx 675$ nm and 1350 nm, respectively, as shown in Fig. 2. These results are similar to the experimental results of a single aperture surrounded by rings^[11].

A nanoslit milled in the metal film can be treated as a metal-insulator-metal (MIM) waveguide. When the Fabry-Perot resonance occurs at the vertical nanoslit region, the SP wave propagates through the MIM waveguide effectively^[16,20]. When the accumulated phase is an even integer of $\pi/2$, the maximum efficiency of the transmission wave through the nanoslit is achieved due to the constructive interference and the minimum efficiency caused by the destructive interference for an odd integer of $\pi/2$ ^[6]. In TM polarized illumination, the transmission efficiency η varies with the metal film thickness t . The transmission efficiency attains the maximum when t holds an integer number of the standing-wave fringes within its depth. Under these circumstances, large amounts of electric charges accumulate at the top and bottom edges of the slit, whereas traveling waves constructively interfere within the MIM waveguide. According to the waveguide theory^[13], the properties of the MIM waveguide are described by σ_x and σ_z . In general, $\sigma_x = \sigma'_x + i\sigma''_x$ and $\sigma_z = \sigma'_z + i\sigma''_z$ are complex numbers, thus encompassing the range of homogeneous and inhomogeneous plane-waves. When a beam propagates along the z -direction in the nanoslit, σ''_z must be

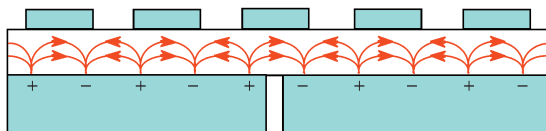


Fig. 3. Distribution of charges and electric fields at the metal and dielectric interfaces.

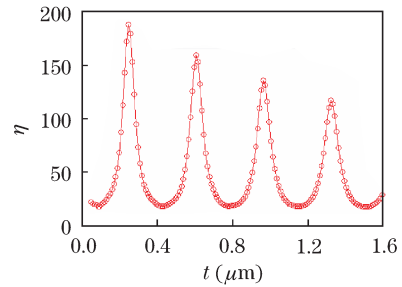


Fig. 4. Transmission efficiencies η through a 50-nm-wide nanoslit as a function of the metal film thickness for a normal incident TM polarized plane wave with wavelength of 1.0 μm .

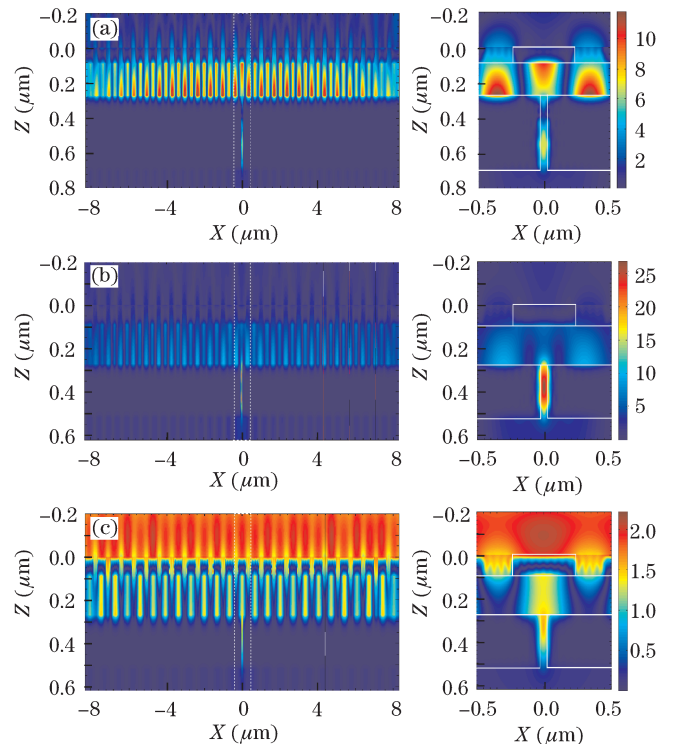


Fig. 5. Distribution of the magnetic field amplitude $|H_y|$ in an enhanced optical transmission structure with a nanoslit milled in metal film with $\Lambda = 675$ nm, $w_s = 475$ nm, $L = 475$ nm, $h = 90$ nm, $d = 180$ nm, $w_p = 50$ nm, $N = 12$. (a) $\lambda_0 = 1.0$ μm , $t = 430$ nm; (b) $\lambda_0 = 1.0$ μm , $t = 250$ nm; (c) $\lambda_0 = 1.5$ μm , $t = 250$ nm. The field distributions of vertical nanoslits are shown in the insets on the right.

positive. In $w_p = 50$ nm, we find $\sigma_z = 1.3910 + 0.0115i$, whose small imaginary part induces a weakly attenuated guided mode. The effective wavelength along the slit is $\lambda_{\text{eff}} = \lambda_0 / \text{Re}(\sigma_z) = \lambda_0 / 1.391 = 719$ nm. The transmission efficiency η simulated by the RCWA method through the nanoslit as a function of the metal film thickness is shown in Fig. 4. The σ_x and σ_z of the MIM waveguide have an imaginary part, causing the transmission efficiency to decay rapidly with the metal film thickness t . If the MIM waveguide is non-absorbing for TM polarization, the transmission efficiency becomes a periodic function of the metal film thickness t . The oscillation period is equal to the wavelength of the standing wave (i.e., a length phase of π) corresponding to the metal film thickness of 0.36 μm . Accordingly, the effective

Table 1. Transmission Efficiency η and the Corresponding Metal Film Thickness t When Optical Transmission Through a Nanoslit Accumulates a Numbered Multiple of $\pi/2$ Phase Difference with $\Lambda = 675$ nm, $w_s = 475$ nm, $L = 475$ nm, $h = 90$ nm, $d = 180$ nm, $w_p = 50$ nm, and $N = 12$

$\Delta\varphi$	Minimum Transmission Efficiencies							
	$\pi/2$	$3\pi/2$	$5\pi/2$	$7\pi/2$	π	2π	3π	4π
t (nm)	90	430	790	1150	250	610	970	1330
η	19.15	15.73	17.86	17.47	187.57	158.89	134.96	116.47

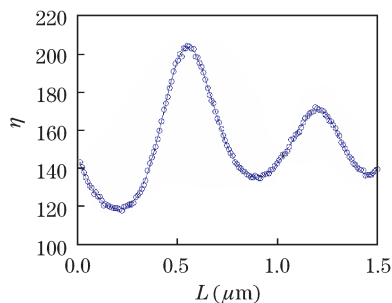


Fig. 6. Transmission efficiency η through a 50-nm-wide nanoslit as a function of the metallic strip width for a normal incident TM polarized plane wave with wavelength of $1.0 \mu\text{m}$.

wavelength inside the slit is $\lambda_{\text{eff}}=720$ nm. Therefore, the wavelength predicted by the standard waveguide theory exhibits good agreement with the results simulated by the RCWA method. Table 1 shows the maximum and minimum transmission efficiencies and their corresponding metal film thicknesses.

When the metal strip period is equal to the SP wavelength, the incident light is coupled into the dielectric interlayer to excite the SP, as shown in Fig. 5(a), where the slit length is $0.43 \mu\text{m}$, and the accumulated phase is $3\pi/2$ for light transmission through the slit. The incident light is coupled into the dielectric interlayer but is not efficiently transmitted through the slit. When the slit length is $0.25 \mu\text{m}$, the Fabry-Perot resonance occurred in the slit, and the incident light is effectively transmitted through the slit, as shown in Fig. 5(b). The maximum transmission efficiency of 187.6 was enhanced. However, if the metallic strip period is mismatched with the SP wavelength (the SP cannot be excited), the incident light is not effectively coupled into the dielectric interlayer with the incident wavelength of $1.5 \mu\text{m}$, as shown in Fig. 5(c).

The metallic strip width over the nanoslit had an influence on the transmission efficiency of waves through the nanoslit due to the disturbance of the nanoslit-generated SP. The transmission efficiency is further improved by optimizing the metallic strip width L over the nanoslit, as shown in Fig. 6. The maximal transmission efficiency of 204.3 is obtained at 550 nm, which is larger than the period metallic strip ridge width of 475 nm.

In conclusion, we present a structure with a 50-nm-wide nanoslit for enhanced optical transmission by coupling light between periodic strips and a metal film due to the presence of excited SP. When the period of the metallic strips is equal to the wavelength of λ_{sp} , the maximum transmission efficiency of 187.6 through the nanoslit is obtained, which is about 24 times than that of the bare resonant nanoslit of 7.8. The metallic strip width L over the nanoslit can be optimized to improve the transmis-

sion efficiency of 204.3.

This work was supported by the Natural Science Foundation Project of CQ CSTC (No. 2010BB2352) and the Chongqing Committee of Education (No. KJ101203). The authors gratefully acknowledge Prof. H. Ming, P. Wang, Y. Lu, Dr. J. Chen (Department of Optics and Optical Engineering, University of Science and Technology of China), Prof. Z. Zhang (G. W. Woodruff school of Mechanical Engineering, Georgia Institute of Technology, and Dr. D. Lu (School of Information Science and Technology, Tsinghua University) for their valuable discussions.

References

1. T. W. Ebbesen, H. J. Lezec, H. F. Ghaemi, T. Thio, and P. A. Wolff, *Nature* **391**, 667 (1998).
2. H. J. Lezec, A. Degiron, R. A. Linke, L. M. Moreno, F. J. Vidal, and T. W. Ebbesen, *Science* **297**, 820 (2002).
3. W. L. Barnes, A. Dereux, and T. W. Ebbesen, *Nature* **424**, 824 (2003).
4. C. Genet and T. W. Ebbesen, *Nature* **445**, 39 (2007).
5. O. T. A. Janssen, H. P. Urbach, and G. W. Hooft, *Phys. Rev. Lett.* **99**, 043902 (2007).
6. T. Thio, H. J. Lezec, T. W. Ebbesen, K. M. Pellerin, G. D. Lewen, A. Nahata, and R. A. Linke, *Nanotechnology* **13**, 429 (2002).
7. D. Cao, H. Zhang, and F. Tao, *Acta Opt. Sin.* (in Chinese) **28**, 1601 (2008).
8. L. Zhou and Y. Zhu, *Acta Opt. Sin.* (in Chinese) **28**, 1047 (2008).
9. H. F. Ghaemi, T. Thio, D. E. Grupp, T. W. Ebbesen, and H. J. Lezec, *Phys. Rev. B* **58**, 6779 (1998).
10. T. Thio, K. M. Pellerin, R. A. Linke, H. J. Lezec, and T. W. Ebbesen, *Opt. Lett.* **26**, 1972 (2001).
11. Z. Liu, Y. Wang, J. Yao, H. Lee, W. Srituravanich, and X. Zhang, *Nano Lett.* **9**, 462 (2009).
12. F. Yang and J. R. Sambles, *Phys. Rev. Lett.* **89**, 063901 (2002).
13. Y. Xie, A. R. Zakharian, J. V. Moloney, and M. Mansuripur, *Opt. Express* **12**, 6106 (2004).
14. M. G. Moharam, E. B. Grann, D. A. Pommet, and T. K. Gaylord, *J. Opt. Soc. Am. A* **12**, 1068 (1995).
15. L. F. Li, *J. Opt. Soc. Am. A* **13**, 1870 (1996).
16. B. J. Lee, L. P. Wang, and Z. M. Zhang, *Opt. Express* **16**, 11328 (2008).
17. Y. Cui and S. He, *Opt. Lett.* **34**, 16 (2009).
18. O. T. A. Janssen, H. P. Urbach, and G. W. 't Hooft, *Opt. Express* **14**, 11823 (2006).
19. Y. Cui, J. He, and S. He, *J. Opt. Soc. Am. B* **26**, 2131 (2009).
20. H. T. Miyazaki and Y. Kurokawa, *Phys. Rev. Lett.* **96**, 097401 (2006).